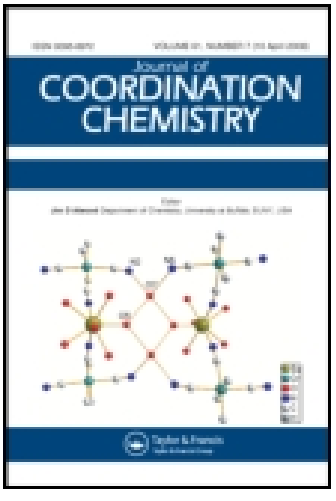

Journal of Coordination Chemistry
Publication details, including instructions for authors and subscription information:
http://www.tandfonline.com/loi/gcoo20

Synthesis, spectroscopic, thermal, and antimicrobial studies of tetradentate 12 and 14 member Schiff bases and their complexes with Fe(III), Co(II), and Cu(II)

Farha Firdaus [a], Kaneez Fatma [a], Mohammad Azam [a] & Mohammad Shakir [a]

[a] Division of Inorganic Chemistry, Department of Chemistry, Aligarh Muslim University, Aligarh 202002, Uttar Pradesh, India

Published online: 29 Oct 2010.

To cite this article: Farha Firdaus, Kaneez Fatma, Mohammad Azam & Mohammad Shakir (2010) Synthesis, spectroscopic, thermal, and antimicrobial studies of tetradentate 12 and 14 member Schiff bases and their complexes with Fe(III), Co(II), and Cu(II), Journal of Coordination Chemistry, 63:22, 3956-3968, DOI: 10.1080/00958972.2010.526707

To link to this article: http://dx.doi.org/10.1080/00958972.2010.526707

Journal of Coordination Chemistry
Vol. 63, No. 22, 20 November 2010, 3956–3968

Synthesis, spectroscopic, thermal, and antimicrobial studies of tetradentate 12 and 14 member Schiff bases and their complexes with Fe(III), Co(II), and Cu(II)

FARHA FIRDAUS*, KANEEZ FATMA, MOHAMMAD AZAM and MOHAMMAD SHAKIR

Division of Inorganic Chemistry, Department of Chemistry, Aligarh Muslim University, Aligarh 202002, Uttar Pradesh, India

(*Received 8 December 2009; in final form 26 July 2010*)

Two Schiff bases, L^1 (5,6;11,12-dibenzophenone-2,3,8,9-tetramethyl-1,4,7,10-tetraazacyclododeca-1,3,7,9-tetraene) and L^2 (6,7;13,14-dibenzophenone-2,4,9,11-tetramethyl-1,5,8,12-tetraazacyclotetradeca-1,4,8,11-tetraene), bearing functionalized pendant arms have been synthesized by cyclocondensation of 3,4-diaminobenzophenone with 2,3-butanedione and 2,4-pentanedione, respectively. Mononuclear macrocyclic complexes $[FeL^1Cl_2]Cl$, $[FeL^2Cl_2]Cl$, $[ML^1Cl_2]$, and $[ML^2Cl_2]$ (where M = Co(II) and Cu(II)) have been prepared by reacting iron(III), cobalt(II), and copper(II) with the preformed Schiff base. The ligands and their corresponding metal complexes were characterized by elemental analyses, ESI-mass spectra, conductivity, magnetic moments, UV-Vis, EPR, IR, ^{1}H-, and ^{13}C-NMR spectral studies, and TGA-DTA/DSC data. The TGA profiles exhibit a two-step pyrolysis, although the iron complexes decompose in three steps, leaving behind metal oxides as the final product. The ligands and complexes were screened *in vitro* against Gram-positive bacteria, Gram-negative bacteria, and fungi.

Keywords: Antimicrobial studies; Pendant arm; Physico-chemical studies; Schiff-base ligands; Thermal studies

1. Introduction

Macrocyclic ligands have received attention due to their ability to discriminate among closely related metal ions based on metal ion radius (ring size effect) [1, 2] and significant enhancement in complex stability constants (macrocyclic effect) [1–3]. Different types of macrocyclic ligands are particularly exciting because of their importance in generating new areas of fundamental and applied chemistry [4]. The most

*Corresponding author. Email: farha_firdaus@yahoo.co.in

ISSN 0095-8972 print/ISSN 1029-0389 online © 2010 Taylor & Francis
DOI: 10.1080/00958972.2010.526707

interesting aspect of macrocyclic ligands are nature, number, and arrangement of the ligand donors as well as ligand conjugation, substitution, and flexibility [5, 6]. The availability of a number of structural derivatives and the ability to complex a large number of metal ions in differing oxidation states have made these ligands attractive for further investigations. Interest in macrocycles with pendant arms is growing for their unique coordination and structural properties, their utility in enzyme-mimicking studies and catalysis and their rapidly growing applications as radiopharmaceuticals, magnetic resonance imaging reagents, and fluorescent probes [7–11]. The chemistry of macrocyclic tetraaza ligands bearing pendant coordinating side arms is a fascinating area of research [12], since such ligands show enhanced thermodynamic and kinetic stabilities due to their modified complexation properties relative to simple macrocyclic precursors [9–13]. Introduction of pendant arms into the macrocyclic framework can enhance the selectivity of the ligand for a given ion and allow for fine-tuning of the properties of the complexes [14]. Properties and coordinating geometries of the complexes of these ligands are influenced by position and number of the functional groups [12]. For N- and C-based macrocyclic ligands, the mode of metal incorporation is very similar to that of metalloproteins in which the requisite metals is bound in a macrocyclic cavity or cleft produced by the conformational arrangement of the protein [11, 15]. A variety of Schiff-base macrocyclic ligands and their complexes have been synthesized [16], prompting us to prepare functionalized macrocyclic ligands, (L^1): 5,6;11,12-dibenzophenone-2,3,8,9-tetramethyl-1,4,7,10-tetraazacyclododeca-1,3,7,9-tetraene and (L^2): 6,7;13,14-dibenzophenone-2,4,9,11-tetramethyl-1,5,8,12-tetraazacyclotetradeca-1,4,8,11-tetraene by condensation of 3,4-diaminobenzophenone with 2,3-butanedione and 2,4-pentanedione, respectively.

2. Experimental

Anhydrous $FeCl_3$, $CoCl_2 \cdot 6H_2O$ and $CuCl_2 \cdot 2H_2O$ (E. Merck) were commercially available as pure samples. The chemicals 2,3-butanedione, 2,4-pentanedione and 3,4-diaminobenzophenone (Fluka) were used as received. Methanol (AR grade) was used as solvent without purification.

2.1. *Synthesis of 5,6;11,12-dibenzophenone-2,3,8,9-tetramethyl-1,4,7,10-tetraazacyclododeca-1,3,7,9-tetraene (L^1)/6,7;13,14-dibenzophenone-2,4,9,11-tetramethyl-1,5,8,12-tetraazacyclotetradeca-1,4,8,11-tetraene (L^2)*

To a stirring methanol solution (25 mL) of 3,4-diaminobenzophenone (3 mmol, 0.636 g), 2,3-butanedione (3 mmol, 0.27 mL)/2,4-pentanedione (3 mmol, 0.31 mL) was added dropwise with constant stirring. The mixture was later refluxed for 12 h. The reaction mixture was allowed to evaporate resulting in isolation of a dark yellow solid on standing for 50 h. The product was filtered off, washed with methanol, and dried in vacuum.

2.2. *Synthesis of complexes, ([FeL^1Cl_2]Cl and [ML^1Cl_2])/([FeL^2Cl_2]Cl and [ML^2Cl_2]) Dichloro[5,6;11,12-dibenzophenone-2,3,8,9-tetramethyl-1,4,7,10-tetraazacyclododeca-1,3,7,9-tetraene]iron(III) chloride and metal chloride/ dichloro[6,7;13,14-dibenzophenone-2,4,9,11-tetramethyl-1,5,8,12-tetraazacyclotetradeca-1,4,8,11-tetraene]iron(III) chloride and metal chloride [M = Co(II) and Cu(II)]*

A methanol solution (25 mL) of L^1 or L^2 (1 mmol) and equimolar amount of metal salt (1 mmol) in methanol (25 mL) were reacted under reflux with constant stirring for 15 h. The reaction mixture thus obtained was continually evaporated leading to isolation of solid products. The product thus formed was filtered, washed several times with methanol, and dried in vacuum.

2.3. *Organism culture and in vitro screening of the ligands and metal complexes*

Antibacterial activity of the synthesized compounds was completed by disc diffusion. The macro-dilution test with standard inoculums of 10^5 CFU mL^{-1} was used to assess the minimum inhibitory concentration (MIC) of the test compounds. DMSO was the solvent. Serial dilutions of the compounds were prepared to the final concentrations of 512, 256, 128, 64, 32, 16, 8, 4, 2, and 1 mg L^{-1}. These tubes were kept at 37°C for 18 h. For assaying antifungal activity, *Candida albicans*, *Candida krusei*, *Candida parapsilosis*, and *Cryptococcus neoformans* were inoculated in Sabouraud Dextrose broth medium (Hi-Media, Mumbai) and incubated for 24 h at 35°C; subsequently, a suspension of 10^6 CFU mL^{-1} was prepared in sterile saline solution according to the McFarland protocol.

2.4. *Physical measurement*

Elemental analyses were recorded on a Perkin Elmer 2400 CHN elemental analyzer; ^{1}H- and ^{13}C-NMR spectra were recorded in DMSO-d_6 using a Bruker Avance II 400 NMR spectrometer from SAIF, Panjab University, Chandigarh, India. FT-IR (4000–200 cm^{-1}) was recorded as KBr/CsI discs on a Perkin Elmer 621 spectrophotometer. ESI-mass spectra were recorded on a Micromass Quattro II Triple Quadruple mass spectrometer. Electronic spectra of the complexes in DMSO were recorded on a Pye-Unicam 8800 spectrophotometer at room temperature. EPR spectra were recorded at room temperature on a Varian E-4 X-band spectrometer using DPPH as the g-marker from SAIF IIT-Madras, Chennai, India. Metals and chlorides were estimated volumetrically [17] and gravimetrically [18], respectively. Magnetic susceptibility measurements were carried out using a Faraday balance at room temperature. The molar conductivity data for 10^{-3} mol L^{-1} solutions in DMSO were recorded on a Systronic type 302 conductivity bridge thermostated at 25.00°C ± 0.05°C. TGA–DTA and DSC were performed on a Shimadzu Thermal Analyzer under nitrogen using alumina powder as reference.

3. Results and discussion

Two functionalized Schiff-base macrocyclic ligands, L^1 and L^2, have been synthesized by condensation between 3,4-diaminobenzophenone and 2,3-butanedione or 2,4-pentanedione in 1 : 1 molar ratio in methanol. The ligands formed are solid and remained unchanged for extended times in air and were found to be soluble in almost all polar solvents. The purities of the ligands and complexes were checked by TLC on silica gel-coated plates using benzene (85%), methanol (10%) and acetic acid (5%) as eluent. Only one spot was observed after developing in an iodine chamber, indicating purity of all the complexes. However, attempts to grow single crystals suitable for X-ray crystallography failed. The formation of these macrocyclic ligand frameworks was confirmed based on elemental analyses, characteristic bands in the FT-IR (table 6), and resonances in the ^{1}H- and ^{13}C-NMR spectra (tables S1 and S2; Supplementary material). The positions of molecular ion peaks in the mass spectra (figures 1 and 2) were consistent with the empirical molecular formula (table 1).

Mononuclear macrocyclic complexes $[FeL^1Cl_2]Cl$, $[FeL^2Cl_2]Cl$, $[ML^1Cl_2]$, and $[ML^2Cl_2]$, where M = Co(II) and Cu(II) (scheme 1), were obtained by reaction of L^1 and L^2 with transition metal ions in 1 : 1 molar ratio. All the macrocyclic complexes are solid, stable to the atmosphere and soluble in polar solvents. Elemental analyses agree well with the suggested macrocyclic frameworks. Formation of tetraimine macrocyclic complexes were further confirmed by mass, FT-IR, ^{1}H- and ^{13}C-NMR data; electronic and electronic paramagnetic resonance spectral studies and magnetic moments gave the geometry around the metal ions.

The thermal analyses and molar conductance data (table 1) of the complexes indicate the non-electrolytic nature of Co(II) and Cu(II) complexes while those for Fe(III) complexes correspond to a 1 : 1 electrolyte [19].

3.1. *In vitro antimicrobial activity of synthesized compounds*

The *in vitro* antibacterial activities of L_1, L_2, and all the complexes were tested using the bacterial cultures of *Streptococcus mutans,* methicillin-resistant *Staphylococcus aureus* (MRSA +ve), *Streptococcus pyogenes*, *Pseudomonas aeruginosa*, *Salmonella typhimurium*, *Escherichia coli* and fungal cultures of *C. albicans*, *C. krusei*, *C. parapsilosis*, and *Cr. neoformans* by the disc diffusion method [20] and then the MICs were determined. Chloramphenicol (30 μg) and fluconazole were used as positive control in the case of bacterial strains and fungi, respectively. The MICs were assessed by the macro-dilution test using standard inoculums of 10^5 CFU mL^{-1}. The susceptibility was assessed on the basis of diameter of zone of inhibition against Gram-positive and Gram-negative strains of bacteria and fungi. The zones of inhibition (mm) of every compound against Gram-positive and Gram-negative strains of bacteria are shown in table 2 and MIC data in table 3. Biological activities show that L^1 and L^2 are biologically active and their metal complexes are more active. L^2 and its complexes were highly active against bacterial strains in comparison to L^1 and its complexes. Cobalt(II) complexes were the best antibacterial complexes while iron(III) and copper(II) complexes were moderate in activity. The MIC confirmed $[CoL^2Cl_2]$ to be the most active. Zones of inhibition for different fungal strains are shown in table 4 and MIC data in table 5. The *in vitro* antifungal activity assay showed that L^1 and its metal complexes were more active than

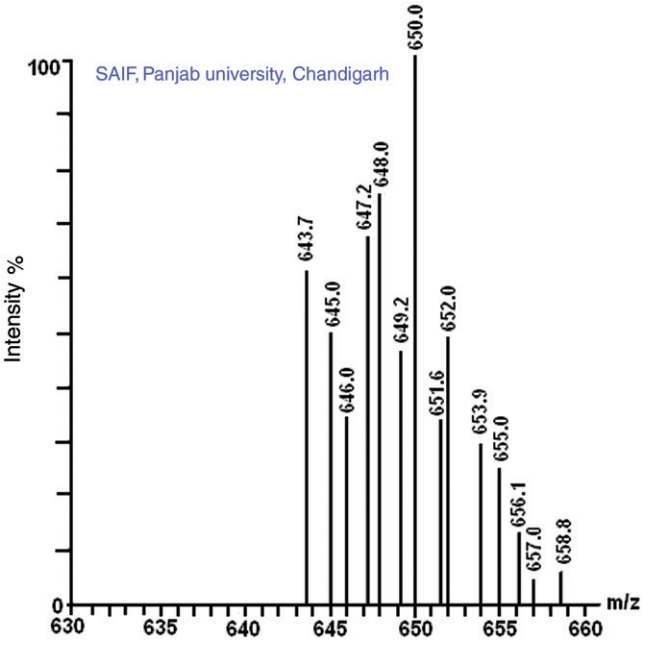

Figure 1. Mass spectrum of $[CuL^1Cl_2]$.

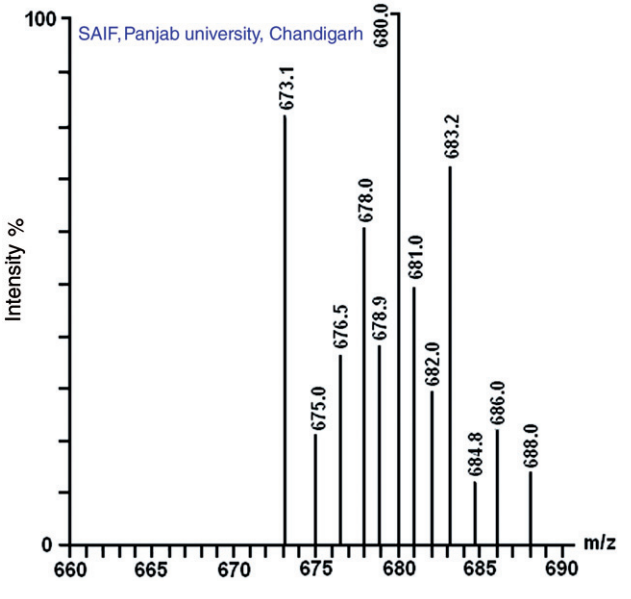

Figure 2. Mass spectrum of $[CuL^2Cl_2]$.

L^2 and its metal complexes. The metal complexes were more active against fungi than the Schiff bases. The cobalt(II) complexes showed moderate activity against all fungal strains, iron(III) complexes show better inhibition and copper(II) complexes show excellent activity against fungal growth.

Table 1. The m/z, color, yield, melting point and molar conductance values of the complexes.

Compounds	m/z found (Calcd)	Color	Yield (%)	Λ_m ($mol^{-1}\,cm^2\,\Omega^{-1}$)	m.p. (°C)
L^1	524.5 (524.6)	Dark yellow	65	–	175
L^2	552.6 (552.6)	Dark brown	68	–	160
$[FeL^1Cl_2]Cl$	686.3 (686.8)	Black	60	50	180
$[FeL^2Cl_2]Cl$	714.6 (714.8)	Black	62	50	180
$[CoL^1Cl_2]$	655.0 (654.4)	Dark yellow	61	20	250
$[CoL^2Cl_2]$	682.2 (682.5)	Black	62	26	280
$[CuL^1Cl_2]$	658.8 (659.0)	Dark brown	55	31	200
$[CuL^2Cl_2]$	688.0 (687.1)	Black	58	18	285

3.2. *Analytical results*

Anal. Calcd for L^1 (%): C, 77.84; H, 5.37; N, 10.67. Found: C, 77.31; H, 5.05; N, 10.15. Anal. Calcd for L^2 (%): C, 78.23; H, 5.83; N, 10.13. Found: C, 77.83; H, 5.51; N, 9.66. Anal. Calcd for $[FeL^1Cl_2]Cl$ (%): Fe, 8.13; Cl, 15.48; C, 59.45; H, 4.10; N, 8.15. Found: Fe, 7.90; Cl, 15.16; C, 59.23; H, 4.00; N, 8.01. Anal. Calcd for $[FeL^2Cl_2]$ Cl (%): Fe, 7.81; Cl, 14.87; C, 68.48; H, 4.51; N, 7.83. Found: Fe, 7.52; Cl, 14.55; C, 68.07; H, 4.22; N, 7.61. Anal. Calcd for $[CoL^1Cl_2]$ (%): Co, 9.00; Cl, 10.83; C, 62.39; H, 4.31; N, 8.56. Found: Co, 8.78; Cl, 10.53; C, 62.07; H, 4.11; N, 8.13. Anal. Calcd for $[CoL^2Cl_2]$ (%): Co, 8.63; Cl, 10.38; C, 63.35; H, 4.72; N, 8.20. Found: Co, 8.41; Cl, 10.06; C, 63.12; H, 4.51; N, 8.00. Anal. Calcd for $[CuL^1Cl_2]$ (%): Cu, 9.64; Cl, 10.75; C, 61.96; H, 4.28; N, 8.50. Found: Cu, 9.22; Cl, 10.43; C, 61.52; H, 4.06; N, 8.10. Anal. Calcd for $[CuL^2Cl_2]$ (%): Cu, 9.24; Cl, 10.31; C, 62.92; H, 4.69; N, 8.15. Found: Cu, 9.00; Cl, 10.10; C, 62.72; H, 4.38; N, 7.81.

3.3. *IR spectra*

The formation of both L^1 and L^2 by condensation of 3,4-diaminobenzophenone and alkyl diketones have been confirmed by the appearance of strong bands at 1645 and 1595 cm^{-1}, characteristic of imine ν(C=N) [21]. The position of this band is shifted by 15–20 cm^{-1} in all metal complexes as compared to free ligands, indicating participation of the imine nitrogen in coordination [22]. The mode of coordination is further supported by the absence of a band at ~3400 cm^{-1}, a characteristic of $\nu(NH_2)$ of 3,4-diaminobenzophenone. The band assigned to pendant carbonyl groups of 3,4-diaminobenzophenone were at 1707–1728 cm^{-1} [23]. Formation of the macrocyclic framework has been further deduced by two sharp bands at 418–426 cm^{-1} and 315–333 cm^{-1} assigned to ν(M–N) and ν(M–Cl), respectively [24]. All the complexes show bands at 2847–2890 cm^{-1} and 1408–1444 cm^{-1} corresponding to ν(C–H) stretching and δ(C–H) bending modes, respectively. Bands corresponding to phenyl ring vibrations appear at their proper positions (table 6).

3.4. *^{1}H-NMR spectra*

The formation of Schiff-base macrocyclic ligands L^1 and L^2 has been further supported by proton magnetic resonance spectra. ^{1}H-NMR spectra of the ligands do not show a

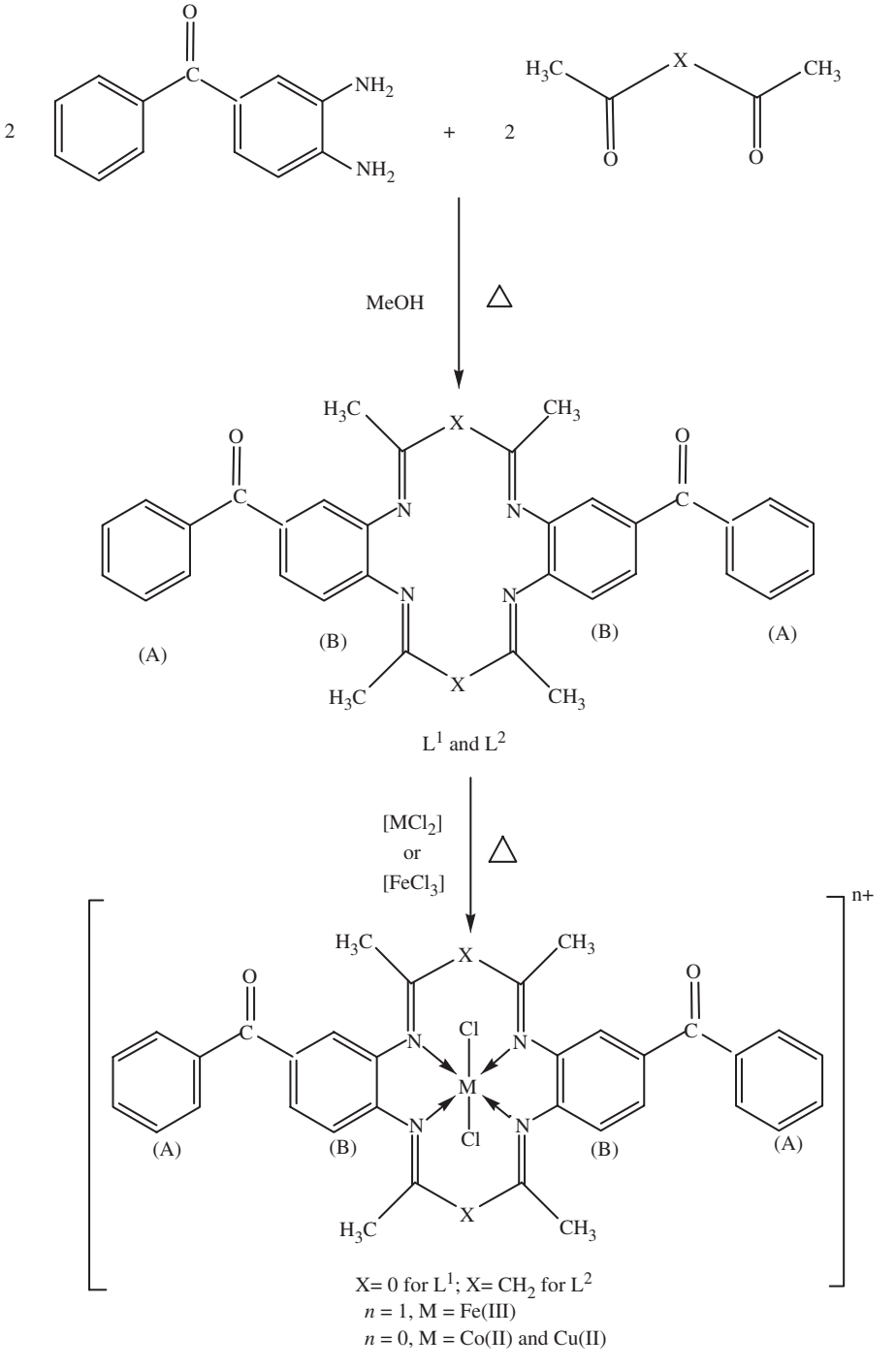

Scheme 1. Preparation and structures of L^1 and L^2 and their metal complexes.

Table 2. Antibacterial activity of the complexes.

Compounds	Gram-positive bacteria			Gram-negative bacteria		
	S. mutans	*S. pyogenes*	*S. aureus*	*P. aeruginosa*	*S. typhimurium*	*E. coli*
L^1	10.9 ± 0.4	10.2 ± 0.8	11.8 ± 0.8	10.3 ± 0.2	10.1 ± 0.5	10.1 ± 0.5
$[FeL^1Cl_2]Cl$	12.9 ± 0.5	12.5 ± 0.3	11.9 ± 0.5	11.5 ± 0.4	10.2 ± 0.5	11.9 ± 0.5
$[CoL^1Cl_2]$	13.5 ± 0.2	14.4 ± 0.1	15.3 ± 0.2	16.1 ± 0.5	17.3 ± 0.2	18.5 ± 0.2
$[CuL^1Cl_2]$	12.3 ± 0.5	12.8 ± 0.3	13.1 ± 0.4	8.8 ± 0.1	14.8 ± 0.2	13.6 ± 0.2
L^2	14.5 ± 0.2	14.3 ± 0.3	14.5 ± 0.5	13.1 ± 0.5	14.1 ± 0.3	15.4 ± 0.2
$[FeL^2Cl_2]Cl$	21.4 ± 0.5	20.1 ± 0.5	19.1 ± 0.2	18.1 ± 0.5	19.2 ± 0.2	21.8 ± 0.5
$[CoL^2Cl_2]$	22.1 ± 0.2	22.3 ± 0.7	21.5 ± 0.4	17.2 ± 0.3	21.4 ± 0.5	23.5 ± 0.4
$[CuL^2Cl_2]$	20.4 ± 0.2	19.3 ± 0.3	19.9 ± 0.3	19.2 ± 0.2	20.4 ± 0.2	21.5 ± 0.2
Chloramphenicol	26.8 ± 0.5	22.4 ± 0.4	21.0 ± 0.5	17.1 ± 0.2	25.2 ± 0.8	20.0 ± 0.2
DMSO	–	–	–	–	–	–

Positive control chloramphenicol and negative control DMSO measured by the Halo Zone Test (Unit, mm).

Table 3. MIC of the complexes, positive control chloramphenicol.

Compounds	Gram-positive bacteria			Gram-negative bacteria		
	S. mutans	*S. pyogenes*	*S. aureus*	*P. aeruginosa*	*S. typhimurium*	*E. coli*
L^1	512	512	512	512	512	512
$[FeL^1Cl_2]Cl$	512	512	512	512	512	512
$[CoL^1Cl_2]$	512	256	256	64	256	64
$[CuL^1Cl_2]$	512	512	512	512	512	512
L^2	512	512	256	512	512	128
$[FeL^2Cl_2]Cl$	128	128	128	32	128	32
$[CoL^2Cl_2$	128	64	64	32	128	32
$[CuL^2Cl_2]$	256	128	128	32	128	32
Chloramphenicol	32	32	32	32	32	32

Table 4. Antifungal activity of the complexes.

Compounds	*C. albicans*	*C. krusei*	*C. parapsilosis*	*Cr. neoformans*
L^1	13.7 ± 0.5	12.8 ± 0.3	12.7 ± 0.3	11.1 ± 0.2
$[FeL^1Cl_2]Cl$	15.6 ± 1.4	14.8 ± 0.2	12.9 ± 0.3	11.8 ± 1.2
$[CoL^1Cl_2]$	14.5 ± 0.5	12.7 ± 0.4	11.8 ± 0.4	10.1 ± 0.5
$[CuL^1Cl_2]$	21.3 ± 1.2	18.6 ± 0.4	17.7 ± 0.4	16.8 ± 0.2
L^2	12.5 ± 0.2	11.5 ± 0.4	11.8 ± 0.2	10.9 ± 0.4
$[FeL^2Cl_2]Cl$	15.5 ± 0.5	13.4 ± 1.2	12.7 ± 0.2	12.6 ± 0.5
$[CoL^2Cl_2]$	12.8 ± 0.2	11.5 ± 0.3	11.4 ± 0.4	10.8 ± 1.2
$[CuL^2Cl_2]$	18.1 ± 0.2	16.2 ± 0.2	15.2 ± 0.2	12.2 ± 0.2
Fluconazole	20.0 ± 0.5	20.0 ± 0.5	18.0 ± 0.5	19.0 ± 0.5
DMSO	–	–	–	–

Positive control (fluconazole) and negative control (DMSO) measured by the Halo Zone Test (Unit, mm)

signal corresponding to primary amino protons of the condensed 3,4-diaminobenzophenone, suggesting that the proposed frameworks have been formed. Spectra of L^1 and L^2 exhibit singlets at 2.15 and 2.19 ppm assigned to methyl protons (CH_3, 12H) [21] of the condensed 2,3-butanedione and 2,4-pentanedione moieties, respectively;

Table 5. MIC of the complexes, positive control fluconazole.

Compounds	*C. albicans*	*C. krusei*	*C. parapsilosis*	*Cr. neoformans*
L^1	32	512	128	512
$[FeL^1Cl_2]Cl$	8	256	128	512
$[CoL^1Cl_2]$	16	512	512	512
$[CuL^1Cl_2]$	2	128	16	32
L^2	32	512	512	512
$[FeL^2Cl_2]Cl$	8	512	128	128
$[CoL^2Cl_2]$	32	512	512	512
$[CuL^2Cl_2]$	4	256	32	128
Fluconazole	1.0	64.0	8.0	8.0

Table 6. IR spectral data (cm^{-1}) of the complexes.

Compounds	ν(C=N)	ν(C=O)	ν(M–N)	ν(C–H)	ν(M–Cl)	Ring vibrations
L^1	1645(s)	1718	–	2868	–	1430, 1092, 728
L^2	1595(s)	1725	–	2880	–	1440, 1098, 735
$[FeL^1Cl_2]Cl$	1620(s)	1722	420(m)	2847	328	1455, 1100, 720
$[FeL^2Cl_2]Cl$	1578(s)	1707	422(m)	2850	333	1460, 1095, 725
$[CoL^1Cl_2]$	1630(s)	1720	426(m)	2890	315	1448, 1105, 732
$[CoL^2Cl_2]$	1575(s)	1728	419(m)	2885	330	1435, 1090, 740
$[CuL^1Cl_2]$	1620(s)	1710	425(m)	2872	320	1458, 1110, 730
$[CuL^2Cl_2]$	1580(s)	1716	418(m)	2860	325	1450, 1108, 738

s, strong intensity band; m, medium intensity band.

a singlet at 3.27 ppm corresponds to methylene protons (C–CH_2–C, 4H) of the condensed 2,4-pentanedione moiety in L^2. Resonances corresponding to various aromatic ring protons [25] appear at their appropriate positions (table S1).

3.5. *^{13}C-NMR spectra*

^{13}C-NMR spectra have strong resonances at 155.6 and 160.0 ppm assigned to imine carbons (C=N) [26] of L^1 and L^2, respectively. Resonances at 22.7 and 18.7 ppm correspond to methyls of L^1 and L^2, respectively. Another resonance at 44.8 ppm is due to methylene carbon of condensed 2,4-pentanedione moiety. Chemical shifts due to 3,4-diaminobenzophenone carbons [27] are listed in table S2.

3.6. *EPR spectra*

EPR spectra of the polycrystalline Cu(II) complexes were recorded at room temperature and at liquid nitrogen temperature and their g and $g_\perp$ values calculated (Supplementary material). Both $[CuL^1Cl_2]$ and $[CuL^2Cl_2]$ exhibit a similar single broad signal (Supplementary material). The absence of hyperfine lines may be due to strong dipolar and exchange interactions between copper(II) ions in the unit cell [28]. The calculated g values of 2.135 and 2.130 and $g_\perp$ values of 2.037 and 2.041 for $[CuL^1Cl_2]$ and $[CuL^2Cl_2]$, respectively, suggest that the unpaired electron is in the $d_{x^2-y^2}$

orbital [29]. The $g > g_{\perp}$ for the complexes show that the unpaired electron is localized in the $d_{x^2-y^2}$ orbital of Cu(II) characteristic of axial symmetry [30]. Tetragonally elongated geometry is thus confirmed [31].

The G values related by the expression $G = (g-2)/(g_{\perp}-2)$ measuring the exchange interaction between metal centers in polycrystalline solids have also been calculated. According to Hathaway and Billing, if $G > 4$ the exchange interaction is negligible, but if $G < 4$, considerable interaction occurs in the complexes [32]. The complexes reported here have G values of 1.048 and 1.043 for $[CuL_1Cl_2]$ and $[CuL_2Cl_2]$, indicating considerable exchange interaction among the Cu(II) ions in these complexes.

3.7. *Electronic spectra and magnetic moments*

Electronic spectra of $[FeL^1Cl_2]Cl$ and $[FeL^2Cl_2]Cl$ show three spectral bands, 17,900 cm^{-1} ($\varepsilon = 51\ L\ mol^{-1}\ cm^{-1}$), 19,900 cm^{-1} ($\varepsilon = 58\ L\ mol^{-1}\ cm^{-1}$), 24,000 cm^{-1} ($\varepsilon = 60\ L\ mol^{-1}\ cm^{-1}$) and 17,200 cm^{-1} ($\varepsilon = 53\ L\ mol^{-1}\ cm^{-1}$), 20,000 cm^{-1} ($\varepsilon = 59\ L\ mol^{-1}\ cm^{-1}$), 23,760 cm^{-1} ($\varepsilon = 63\ L\ mol^{-1}\ cm^{-1}$), which may be assigned to $^6A_{1g} \rightarrow {}^4T_{1g}$, $^6A_{1g} \rightarrow {}^4T_{2g}$, $^6A_{1g} \rightarrow {}^4A_{1g}$, ^4E_g transitions, respectively. These bands are consistent with octahedral geometry [33] around Fe(III), which is further supported by the observed magnetic moment of 5.9 B.M. for $[FeL^1Cl_2]Cl$ and 5.8 B.M. for $[FeL^2Cl_2]Cl$.

Electronic spectra of the cobalt complexes exhibit two absorption bands at 8100 cm^{-1} ($\varepsilon = 13\ L\ mol^{-1}\ cm^{-1}$), 16,700 cm^{-1} ($\varepsilon = 17\ L\ mol^{-1}\ cm^{-1}$) for $[CoL^1Cl_2]$ and 9160 cm^{-1} ($\varepsilon = 12\ L\ mol^{-1}\ cm^{-1}$), 17,240 cm^{-1} ($\varepsilon = 15\ L\ mol^{-1}\ cm^{-1}$) for $[CoL^2Cl_2]$, comparable to the characteristic features of distorted octahedral Co(II) complexes [34], which may be reasonably assigned to $^4T_{1g}(F) \rightarrow {}^4T_{2g}(F)$ (ν_1) and $^4T_{1g}(F) \rightarrow {}^4A_{2g}(F)$ transitions. The observed magnetic moments of 4.8 and 4.9 B.M. further complement the electronic spectral findings.

Electronic spectra of Cu(II) complexes show bands at 13,899 cm^{-1} ($\varepsilon = 30\ L\ mol^{-1}\ cm^{-1}$) and 16,720 cm^{-1} ($\varepsilon = 45\ L\ mol^{-1}\ cm^{-1}$) for $[CuL^1Cl_2]$ and 14,012 cm^{-1} ($\varepsilon = 33\ L\ mol^{-1}\ cm^{-1}$) and 16,600 cm^{-1} ($\varepsilon = 49\ L\ mol^{-1}\ cm^{-1}$) for $[CuL^2Cl_2]$. These may be assigned to $^2B_{1g} \rightarrow {}^2A_{1g}$ and $^2B_{1g} \rightarrow {}^2E_g$ transitions, respectively. Because of low intensity of $^2B_{1g} \rightarrow {}^2B_{2g}$, this band is usually not observed as a separate band in tetragonally distorted complexes [35]. The geometry of the Cu(II) complexes is further supported by the magnetic moment values [24] of 1.8 and 1.9 B.M. for $[CuL^1Cl_2]$ and $[CuL^2Cl_2]$, respectively.

3.8. *Thermal analysis by TGA–DTA/DSC*

The observed percentage weight losses corresponding to various steps in all thermograms are compared with those calculated [36]. The TGA of L^1 and L^2 consist of two well-defined stages. The first starts at 250–329°C and 200–358°C in L^1 and L^2, respectively, corresponding to degradation of two pendant groups ($2C_7H_5O$) contributing 39.72% (Calcd 40.07%) and 38% (Calcd 38.03%) weight loss of L^1 and L^2, respectively. The initial decomposition of the exocyclic rings is common in such complexes [37]. The second stage from 402°C to 650°C and 440–670°C consists of

degradation of the remaining part with estimated loss of 59.32% (Calcd 60.28%) and 61.63% (Calcd 62.00%) in L^1 and L^2, respectively.

The DTA curves of L^1 and L^2 show endothermic peaks at 347°C and 525°C, respectively, which may be assigned to loss of pendant moieties. Other endothermic peaks at 543°C and 649°C correspond to decompositions of the whole L^1 and L^2, respectively.

The DSC profiles of L^1 and L^2 exhibit exothermic peaks at 245–325°C and an endothermic peak at 500–569°C due to pyrolysis of the whole organic moiety.

The metal complexes exhibit similar thermal decompositions. Complexes of Co(II) and Cu(II) show two stage thermograms, 280–447°C and 507–685°C. The first stage accounts for 11% weight loss corresponding to the removal of chlorides and the second stage is consistent with degradation of the remaining compound. TGA of Fe(III) complexes show three well-defined stages. The first stage at 170–190°C continuing to 200–248°C corresponds to loss of one chloride outside the coordination sphere (4.92%, Calcd 5.16% and 4.73%, Calcd 4.95%) in $[FeL^1Cl_2]Cl$ and $[FeL^2Cl_2]Cl$, respectively. The second stage between 300°C and 410°C may be due to loss of two coordinated chlorides corresponding to 9.98% (Calcd 10.88%) and 10.01% (Calcd 10.88%) and the final peak 585–700°C may be assigned to the loss of organic ligand in $[FeL^1Cl_2]Cl$ and $[FeL^2Cl_2]Cl$. TGA curves of all the complexes show a straight horizontal line even on heating to 850°C indicating formation of metal oxide residue [38].

The DTA curves of the complexes show endothermic peaks at 313–440°C assigned to loss of coordinated chlorides. The broad endothermic peak obtained between 501°C and 638°C is due to decomposition and formation of metal oxides. The DTA of $[FeL^1Cl_2]Cl$ and $[FeL^2Cl_2]Cl$ complexes exhibit a small endotherm at 195°C and 230°C, respectively, due to loss of one chloride outside the coordination sphere.

In the DSC plots, a small endothermic peak at 296–320°C is due to liberation of chlorides, while endothermic peak at 399–450°C is due to pyrolysis of the whole moiety with well-defined exotherms at 505–595°C corresponding to formation of metal oxides [39]. Strictly horizontal levels between 450°C and 500°C are not possible for $[FeL^1Cl_2]Cl$ and $[FeL^2Cl_2]Cl$ due to loss of iron chloride. A new level extending from 500°C to 600°C corresponding to ferric oxide was observed. These oxides decompose at high temperature and regain their initial weight at 811°C.

4. Conclusion

Iron(III), cobalt(II), and copper(II) complexes with two Schiff-base ligands, L^1 and L^2, bearing functionalized pendant arms have been synthesized by cyclocondensation of 3,4-diaminobenzophenone with 2,3-butanedione and 2,4-pentanedione. The synthesized Schiff bases are tetradentate through coordination of azomethine to metal. Octahedral geometry for Fe(III) complexes and distortion from octahedral geometry for Co(II) and Cu(II) complexes have been assigned on the basis of elemental, thermal, and spectral data. The antimicrobial activities of all the complexes indicate that they are active against a series of pathogens and the metal complexes are more active than their respective parent ligands.

Acknowledgments

The authors acknowledge The Chairman, Department of Chemistry, Aligarh Muslim University, Aligarh, India for providing necessary research facilities. They are grateful to Dr Asad Ullah Khan, Interdisciplinary Biotechnology Unit, Aligarh Muslim University, Aligarh for performing antimicrobial activity and SAIF, Panjab University Chandigarh, India for providing, NMR and elemental analysis, and to SAIF IIT-Madras, Chennai, India for performing EPR spectra. They thank Prof. R.J. Singh, Department of Physics, AMU, Aligarh for the discussion of EPR spectra.

References

[1] T.E. Jones, L.L. Zimmer, L.L. Diaddario, D.B. Rorabacher. *J. Am. Chem. Soc.*, **97**, 7163 (1975).
[2] V.J. Thom, J.C.A. Boeyens, G.J. McDougall, R.D. Hancock. *J. Am. Chem. Soc.*, **106**, 3198 (1984).
[3] R.D. Hancock, S.M. Dobson, A. Evers, P.W. Wade, M.P. Ngwenya, J.C.A. Boeyens, K.P. Wainwright. *J. Am. Chem. Soc.*, **110**, 2788 (1988).
[4] J.M. Lehn. *Supramolecular Chemistry, Concepts and Perspectives*, VCH, Weinheim (1995).
[5] K.R. Adam, D.S. Baldwin, P.A. Duckworth, L.F. Lindoy, M. McPartlin, A. Bashall, H.R. Powell, P.A. Tasker. *J. Chem. Soc., Dalton Trans.*, 1127 (1995).
[6] P.M. Reddy, A.V.S.S. Prasad, K. Shanker, V. Ravinder. *Spectrochim. Acta, Part A*, **68**, 1000 (2007).
[7] T.A. Kaden. *Pure Appl. Chem.*, **65**, 1477 (1993).
[8] K.P. Wainwright. In *Advances in Inorganic Chemistry*, A.G. Sykes (Ed.), Vol. 52, pp. 293–334, Academic Press, San Diego (2001).
[9] S.G. Kang, S.J. Kim. *Bull. Korean Chem. Soc.*, **24**, 269 (2003).
[10] V. Comblin, D. Glisoul, M. Hermann, V. Humblet, V. Jacques, M. Mesbahi, C. Sauvage, J.F. Desreux. *Coord. Chem. Rev.*, **185–186**, 451 (1999).
[11] J. Costamagna, G. Ferraudi, B. Matsuhiro, M. Compos-Vallette, J. Canales, M. Villagran, J. Vargas, M.J. Aruirre. *Coord. Chem. Rev.*, **196**, 125 (2000).
[12] H. Aneetha, Y.H. Lai, S.C. Lin, K. Panneerselvam, T.H. Lu, C.S. Chung. *J. Chem. Soc., Dalton Trans.*, 2885 (1999).
[13] X. Sun, M. Wuest, G.R. Weisman, E.H. Wong, D.P. Reed, C.A. Boswell, R. Motekaitis, A.E. Martell, M.J. Welch, C.J. Anderson. *J. Med. Chem.*, **45**, 469 (2002).
[14] E. Maimon, I. Zilbermann, G. Golub, A. Ellern, A.I. Shames, H.A. Cohen, D. Meyerstein. *Inorg. Chim. Acta*, **324**, 65 (2001).
[15] E.Q. Gao, H.Y. Sun, D.Z. Liao, Z.H. Jiang, S.P. Yan. *Polyhedron*, **21**, 359 (2002).
[16] N.E. Borisova, M.D. Reshetova, Y.A. Ustynyuk. *Chem. Rev.*, **107**, 46 (2007).
[17] C.N. Reilly, R.W. Schmid, F.A. Sadak. *J. Chem. Educ.*, **36**, 619 (1959).
[18] A.I. Vogel. *A Text Book of Quantitative Inorganic Analysis*, 3rd Edn, pp. 433–434, Longman, London (1961).
[19] W.J. Geary. *Coord. Chem. Rev.*, **7**, 82 (1971).
[20] S.A. Khan, K. Saleem, Z. Khan. *Eur. J. Med. Chem.*, **42**, 103 (2007).
[21] N. Raman, C. Thangaraja. *Transition Met. Chem.*, **30**, 317 (2005).
[22] N. Gupta, R. Gupta, S. Chandra, S.S. Bawa. *Spectrochim. Acta, Part A*, **61**, 1175 (2005).
[23] O.Z. Yesilel, H. Olmez. *Transition Met. Chem.*, **30**, 992 (2005).
[24] S. Chandra, Sangeetika. *Spectrochim Acta, Part A*, **60**, 2153 (2004).
[25] P.V.G. Reddy, Y.B.R. Kiran, C.S. Reddy, C.D. Reddy. *Chem. Pharm. Bull.*, **52**, 307 (2004).
[26] M. Shakir, N. Begum, S. Parveen, P. Chingsubam, S. Tabassum. *Synth. React. Inorg. Met-Org. Chem.*, **34**, 1135 (2004).
[27] P.V.G. Reddy, C.S. Reddy, C.N. Raju. *Chem Pharm. Bull.*, **51**, 860 (2003).
[28] I.S. Ahuja, S. Tripathi. *Ind. J. Chem.*, **30(A)**, 1060 (1991).
[29] F.K. Kneubuhl. *J. Chem. Phys.*, **33**, 1074 (1960).
[30] D. Kivelson, R. Neiman. *J. Chem. Phys.*, **35**, 149 (1961).
[31] S. Chandra, L.K. Gupta. *Spectrochim. Acta, Part A*, **60**, 2767 (2004).
[32] B.J. Hathaway, D.E. Billing. *Coord. Chem. Rev.*, **5**, 143 (1970).
[33] C.J. Ballhausen. *Introduction to Ligand Field Theory*, McGraw-Hill, New York (1962).
[34] D.P. Singh, R. Kumar, V. Malik, P. Tyagi. *J. Enzyme Inhib. Med. Chem.*, **22**, 177 (2007).

[35] K.G. Kocwin, W. Wojciechowski. *Transition Met. Chem.*, **21**, 312 (1996).
[36] J. Bassett, R.C. Denney, G.H. Jeffrey, J. Mendham. *Vogels Textbook of Quantitative Inorganic Analysis*, 4th Edn, Longman, London (1978).
[37] X. Wei, X. Du, D. Chen, Z. Chen. *Thermochim. Acta*, **440**, 181 (2006).
[38] A.A. Ahmed, S.A. BenGuzzi, A.A. El-Hadi. *J. Sci. Appl.*, **1**, 79 (2007).
[39] S.M. Annigeri, A.D. Naik, U.B. Gangadharmath, V.K. Revankar, V.B. Mahale. *Transition Met. Chem.*, **27**, 316 (2002).